Radial Segregation in a Two-Dimensional Rotating Drum

Christian M. Dury and Gerald H. Ristow (*)

Fachbereich Physik, Philipps-Universität Marburg, Renthof 6, 35032 Marburg, Germany

(Received 19 August 1996, received in final form 23 December 1996, accepted 16 January 1997)

PACS.64.75.+g – Solubility, segregation, and mixing; phase separation
PACS.83.70.Fn – Granular solids
PACS.02.70.Ns – Molecular dynamics and particle methods

Abstract. — We simulate the size segregation of a binary mixture of granular material in a half filled two-dimensional rotating drum using the discrete elements method with linear contact forces. The dynamics of the segregation process is studied in detail as function of the angular velocity of the drum. We propose an order parameter to characterize the final amount of segregation and the segregation speed which allows to compare systems of different sizes and with different material properties. We demonstrate its usefulness by investigating its time dependence as function of the angular velocity of the drum and discuss the interplay between the thickness of the flowing layer and the mean particle velocity.

1. Introduction

The behavior of granular materials is of great technological interest [1], and its investigation has a history of more than two hundred years. Nevertheless the basic physical understanding of granular media is far from being complete. One of their most intriguing properties is their tendency to segregate which is observed in many industrial particle handling situations, such as transporting grains or mixing pharmaceutical pills [2]. The rotating-cylinder geometry is an archetype of numerous devices used in industrial material processing where radial segregation [2–4] can occur on short time scales and axial segregation is observed on larger time scales [5]. The mechanism of the segregation process is based on the surface flow where small particles get stuck along the inclined plane more likely than the larger ones, hence accumulating near the center of the rotating drum. It was argued *e.g.* by Hill and Kakalios [5] that the angle of repose for different materials or mixtures is the triggering mechanism for axial segregation but this could not be verified (within the error bars) by experiments in a two-dimensional rotating drum using disks of various sizes [6]. Many parameters are involved in the process of radial segregation and mixing, such as size, shape, mass [7], frictional forces, angular velocity, filling of the drum [8,9], *etc.* In this paper we focus on the dependence of the angular velocity. We are studying the segregation velocity of a half filled bidimensional drum rotating with an angular velocity ω with radius R. The drum is filled with a binary mixture of particles where the radii of the small particles are r_S and the radii of the larger ones are r_L. The first part of our paper describes the numerical methods and parameters we use. In the second part

(*) Author for correspondence (e-mail: ristow@stat.physik.uni-marburg.de)

a quantitative analysis of the segregation for different rotational velocities will be given and the interplay of the thickness of the fluidized layer and the mean particle velocity within it will be discussed.

2. Model

In order to study our system with computer simulations we use molecular dynamics for granular materials also known as discrete element method (DEM) [10]. In experiments with mustard seeds in a rotating drum one observes that most of the particles in the fluidized layer are sliding and not rotating [11]. In order to approximate these conditions we use spherical particles with no rotation instead of elliptical particles with rotation. To avoid close-packed structures we use particles with different sizes in our simulation. Whenever two particles i and j are closer than the sum of their radii particle j exerts a force on particle i and *vice versa.*

2.1. NORMAL FORCE. — For the force in normal direction we use linear interactions with damping:

$$F_{ij}^N = -k_n r_{\text{eff}}(|\mathbf{x}_i - \mathbf{x}_j| - (r_i + r_j)) - \gamma_n m_{\text{eff}}(\mathbf{v}_i - \mathbf{v}_j)\hat{\mathbf{n}}.$$

Here $\mathbf{x}_i, \mathbf{v}_i$ denotes the position and velocity of particle i and $\hat{\mathbf{n}}$ is the unit vector in normal direction $\hat{\mathbf{n}} \parallel (\mathbf{x}_i - \mathbf{x}_j)$. The radius of particle i is r_i and $r_{\text{eff}}, m_{\text{eff}}$ are the reduced radius and mass of the two particles. The stiffness of the material is characterized by k_n and γ_n and is directly related to the coefficient of restitution ϵ_{res} *via*:

$$\epsilon_{\text{res}} = \exp\left[-\frac{\gamma_n}{2} t_c\right]$$

where t_c is the contact time of the two colliding particles:

$$t_c = \frac{\pi}{\sqrt{(k_n r_{\text{eff}}/m_{\text{eff}}) - (\gamma_n/2)^2}}.$$

The algorithm is stable for a time step of $\mathrm{d}t < t_c/8$; to be on the save side we choose the time step to be $\mathrm{d}t := t_c/15$. In order to save computer time, we set k_n to 10^8 Pa which is about one order of magnitude softer than vulcanite but the maximal overlap of two particles was at most 0.3% of the sum of their radii, which is still realistic. To suppress particle bouncing on the surface, which could disturb the segregation we choose the damping coefficient γ_n to give $\epsilon_{\text{res}} = 28.7\%$. The coefficient of restitution has also an effect on the angle of repose, shown in Figure 1. With decreasing ϵ_{res} the angle of repose in the rotating drum increases strictly monotonically. The parabolic fit to the data points gives an extrapolated value of 39° in the limit $\epsilon_{\text{res}} \to 0$. For these values of our parameters the time step is $\mathrm{d}t = 0.85 \times 10^{-6}$ s.

2.2. SHEAR FORCE. — For the shear force we put upon contact a linear spring between the two particles which results in a restoring force. If the restoring force would be larger than Coulomb's frictional force the spring is cut and we switch to sliding friction with Coulomb's law

$$F_{ij}^{\text{S}} = -\text{sign}\left((\mathbf{v}_i - \mathbf{v}_j)\hat{\mathbf{s}}(t)\right) \min\left(k_{\text{s}} \int (\mathbf{v}_i - \mathbf{v}_j)\hat{\mathbf{s}}(t)\mathrm{d}t, \mu |F_{ij}^N|\right).$$

Here $\hat{\mathbf{s}}$ is the unit vector in shear direction $\hat{\mathbf{s}} \perp \hat{\mathbf{n}}$. With this frictional law we do not need to have an artificial roughening of the boundary walls to have static friction.
For the friction coefficient μ we have $\mu = 0.4$ and for the spring constant k_{s} of the tangential spring we use $k_{\text{s}} = 100$ Pam.

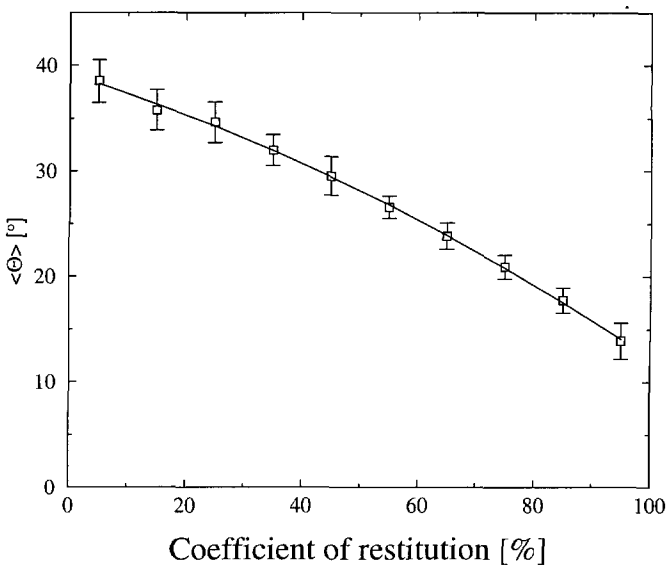

Fig. 1. — The dependence of the angle of repose $\langle\theta\rangle$ on the coefficient of restitution ϵ_{res} for an angular velocity of $\omega = 2$ Hz. The solid line is a parabolic fit to the data points.

2.3. PARAMETERS. — In our simulation we use a binary mixture of $N = 1\,600$ particles with radius $r_{\text{S}} = 0.038$ cm and $r_{\text{L}} = 0.064$ cm, the fraction of the small particles is $f = 45\%$. Our drum with radius $R = 3.5$ cm is half filled and the packing fraction is $\eta = 0.77$. The particles and the inner wall of the drum are made of the same material described by the parameters above.

3. Rotating Drum

We are starting with a half filled drum in order to minimize the effect of mixing [8,9] shown in Figure 2a and then let the drum rotate with angular velocity ω. We choose ω in a region with continuous surface flow just above where we would get distinct avalanches [12]. After some revolutions we get a clearly segregated core composed out of small particles drawn as black circles shown in Figure 2b. In order to characterize the segregation quantitatively we investigate the density of small particles at a given distance r from the center of the drum which is similar to the method used in [13].

3.1. DENSITY PROFILE. — To obtain the density profile for small particles we divide the disc segment into concentric shells with width Δ and inner radius $R_i = i\Delta$ of shell i where $i = 0, 1, . \quad , (R/\Delta) - 1$. To quantify the quality of the segregation we normalize the measured density by dividing by $\rho_{\text{S}} = \eta/(\pi r_{\text{s}}^2)$ which is the theoretical density if only small particles were present. The probability density $\rho_\Delta(R_i)$ is thus defined as:

$$\rho_\Delta(R_i) := \frac{\pi r_{\text{s}}^2}{\eta} n_\Delta(R_i).$$

Here $n_\Delta(R_i)$ is the number of small particles in shell i with width Δ divided by the area $A = \frac{1}{2}\left[(R_i + \Delta)^2 - R_i^2\right]\pi$ of shell i. $\rho_\Delta(R_i)$ ranges from 0 to 1 and in the unsegregated case

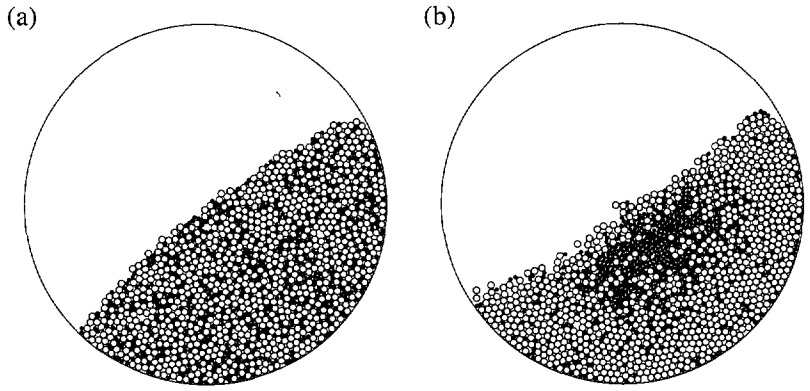

Fig. 2. — 2D-drum: small particles are drawn as filled circles and large particles as open circles. a) Snapshot of the drum right before the first avalanche. b) Snapshot of the drum after rotating $t = 60$ s with angular velocity $\omega = 1.0$ Hz, *i.e.* after 9 rotations.

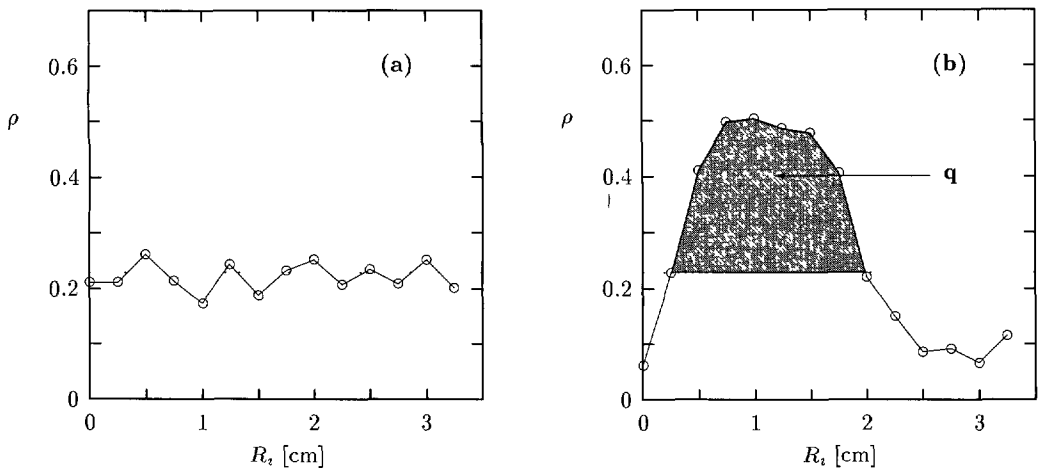

Fig. 3. — Density profiles for Figure 2: a) at $t = 0$ s; b) after segregation, giving a value of $q = 0.39$. The dotted line denotes the density for the unsegregated case ρ_0.

the probability density is in all shells $(2fN/\eta)\,(r_s/R)^2$ which gives for our values $\rho_0 = 0.228$. In Figure 3a we show the density profile of Figure 2a and the dotted line denotes ρ_0. The density profile fluctuates around ρ_0 as expected. In Figure 3b the density profile of the configuration in Figure 2b is given, here one can clearly see the segregated core of the small black particles where the value of ρ is approximately 0.5. On top of the core, $R_i < 0.25$ cm, we can see the fluidized layer composed of large and small particles. The probability density for our segregated configuration cannot reach the maximum possible value of one, because the segregated core of small particles is not really a half disk and on top of it there is always a fluidized zone which is composed also out of large particles. Therefore the maximum realistic possible value for ρ is about 0.7. Further away from the center of the drum, $R_i \geq 2$ cm, the density of the small particles is below the value of the unsegregated case and even drops to less than $\rho_0/2$ for $R_i = 3$ cm. In this region the larger particles concentrate as already visible in Figure 2b. It is

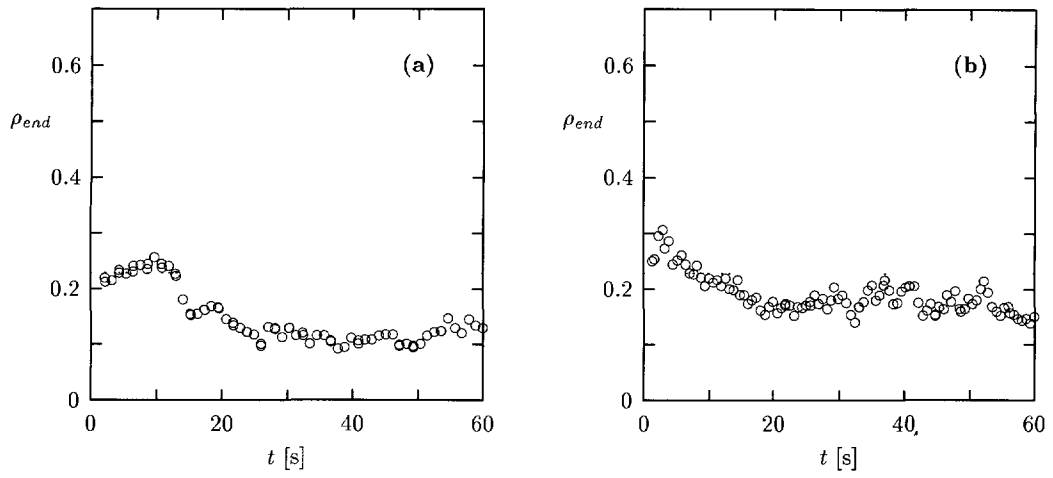

Fig. 4. — Evolution of the density of small particles at the outer most shell: a) $\omega = 0.75$ Hz and b) $\omega = 2.5$ Hz. The dotted line denotes the density for the unsegregated case ρ_0.

interesting to note that right at the wall boundary the density of small particles increases again which we found in all our simulations for different model parameter k_s, μ, γ_n and regardless of the angular velocity of the drum. Its height $\rho_{\text{end}} := \rho_\Delta(R - \Delta)$ seems to be related to the quality of the segregation since values of ρ_{end} close to or above ρ_0 always gave not well segregated cores. This could be due to some finite size effects and depends on the thickness of the fluidized zone. Even though the angle of repose is nearly constant in our range of ω [12], $\Theta \approx 33°$, the thickness of the fluidized zone grows with ω [14, 15] and so the small particles cannot segregate fast enough through the fluidized layer to the solid block and will end up at the wall. In Figure 4, we show the time evolution of ρ_{end} for two different angular velocities $\omega = 0.75$ Hz (a) and $\omega = 2.5$ Hz (b), respectively. For lower values of ω, the depletion of the small particles in the outermost shell is faster and the final value around which ρ_{end} fluctuates is lower. This indicates that the maximal achievable amount of segregation is higher for smaller ω which will be verified and quantified in the next section using an appropriate order parameter.

3.2. Order Parameter. — To compare the quality and speed of the segregation of different runs with different parameters it is desirable to have only one order parameter to investigate. We choose as such an order parameter q the sum over all positive deviations of $\rho_\Delta(R_i)$ above the mean ρ_0 normalized with respect to the ideally segregated case, where all inner shells $i = 0, .., c$ are composed only out of small particles and in the outer shells $i = c+1, .., (R/\Delta)-1$ there are only large particles. To illustrate this procedure, we have shaded the area that enters our calculations in Figure 3b. In the ideally segregated case the inner half disk has radius of $R_c = r_s\sqrt{2fN/\eta}$ which gives for our values $R_c = 1.64$ cm. Cast into a formula, we define our order parameter q as:

$$q := \frac{1}{c_n} \sum_{i=0}^{(R_c/\Delta)-1} (\rho_\Delta(R_i) - \rho_0)\, \Theta\left(\rho_\Delta(R_i) - \rho_0\right),$$

with $\Theta(x)$ as the Heaviside Step function. For calculating the normalization constant c_n we choose for convenience the width of the shells Δ to be an integer fraction of the drum radius R and of R_c. So we get for the probability density in the ideally segregated case

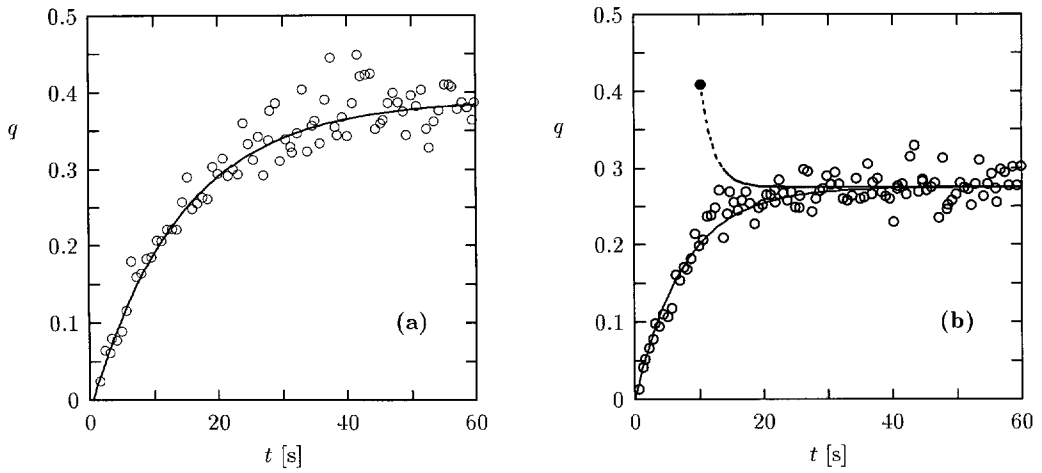

Fig. 5. — Time evolution of our order parameter $q(t)$. a) For $\omega = 0.75$ Hz. The solid line is the fitted curve with $q_\infty = 0.395$ and $\tau = 15.4$ s. b) For $\omega = 2.5$ Hz. The solid line is the fitted curve with $q_\infty = 0.275$ and $\tau = 7.7$ s and the dotted line is the time evolution of a more segregated initial configuration.

$\rho_{S\Delta}(R_i) = \Theta(R_c - R_i)$ and the normalization constant c_n is:

$$c_n := \sum_{i=0}^{R/\Delta} (1-\rho_0)\Theta(R_c - R_i) = (1-\rho_0)\frac{R_c}{\Delta} = \left(1 - \frac{r_s^2}{R^2}\frac{2fN}{\eta}\right)\frac{r_s}{\Delta}\sqrt{\frac{2fN}{\eta}}.$$

In Figure 5 we compare the time evolution of the order parameter $q(t)$ for runs with different angular velocities and find that $q(t)$ saturates in both cases. The fluctuations of the order parameter in the saturated phase are also seen in experiments [3] and are therefore most probably not an artifact of our method. Both graphs can easily be fitted to an exponential law of the form:

$$q(t) = q_\infty \left(1 - \mathrm{e}^{-t/\tau}\right)$$

where q_∞ denotes the quality of the segregation (or final amount of segregation) and τ the characteristic segregation time. When using the data given in Figure 5b, we get for $\omega = 0.75$ Hz (a) values of $q_\infty = 0.395$ and $\tau = 15.4$ s whereas for $\omega = 2.5$ Hz (b) values of $q_\infty = 0.275$ and $\tau = 7.7$ s. This states that even though the initial segregation speed is higher for higher values of ω, the final amount of segregation is less. In order to half the characteristic segregation time τ, ω has to be increased by a factor of 3. Also shown in Figure 5b as dotted line is a test run where we started with a more segregated configuration. The value of q decreases in time and verifies that the order parameter indeed does not reach a value of 1 but rather approaches q_∞.

3.3. Dynamics of the Segregation Process. — But what is the exact dependence of the quality of the segregation and the characteristic segregation time on the angular velocity of the rotating drum? We start with a rotating speed ω just above the distinct avalanche regime [12] which gives $\omega = 0.5$ Hz for our simulation parameters and increase ω in steps of 0.25 Hz up to 2.5 Hz. The corresponding values of q_∞ and τ are given as function of ω in Figures 6a and b, respectively. With increasing ω, q_∞ decreases only slightly in the beginning up to $\omega = 1$ Hz but for higher values of ω the decrease becomes more pronounced. The segregation mechanism is

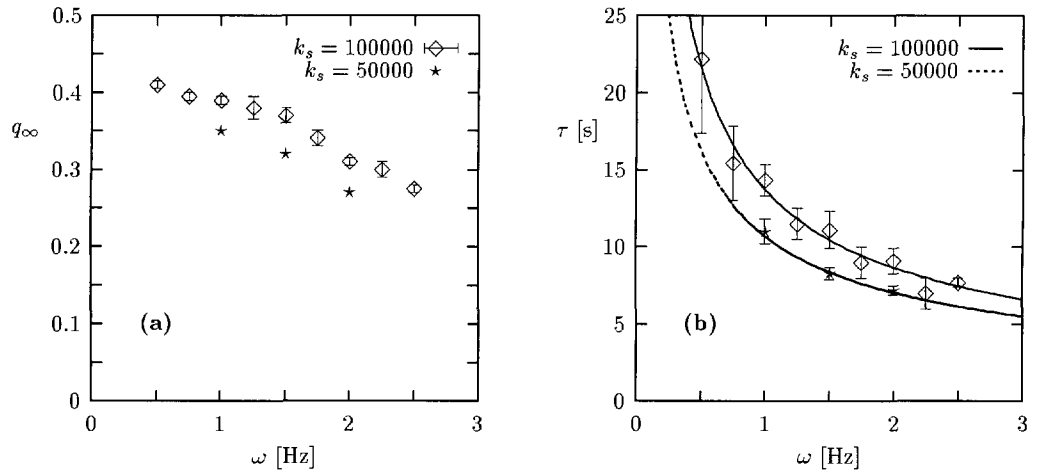

Fig. 6. — Dependence on the angular velocity of $q(t,\omega)$: a) the coefficient $q_\infty(\omega)$ for the quality of the segregation, b) the coefficient $\tau(\omega)$ for the characteristic segregation time. The solid line corresponds to $\tau(\omega) = 13.7\ \omega^{-2/3}$

based on the surface flow and with no surface flow there is no segregation. Therefore it is clear that in the limit $\omega \to 0$ we get $\tau \to \infty$, because for lower and lower ω we are in the discrete avalanche regime and the separation of the avalanches grows more and more. The best fit for $\tau(\omega)$ by a power law gives:

$$\tau(\omega) = 13.7\ \omega^{-0.66}$$

The natural time scale for the segregation process is the average frequency a particle is exposed to the surface, *i.e.* the number of revolutions. Defining $n_R := \tau(\omega)\omega/(2\pi)$, we can rewrite the above equation for $\tau(\omega)$ and obtain

$$n_R = 2.18\ \omega^{0\,33},$$

which is shown in Figure 7a as solid line where the data points from Figure 6b are replotted in this dimensionless fashion. One can see that for higher ω we need more revolutions to achieve segregation.

In order to discuss the influence of the thickness of the fluidized layer on the characteristic segregation time $\tau(\omega)$, we vary our simulation parameter k_s which is related to the surface roughness of the material being used. How this influences the layer thickness d_f is shown in Figure 7b as function of ω for the three different values $k_s = 50\,000(\star), 100\,000(\circ)$ and $150\ 000(\bullet)$. The thickness increases with decreasing k_s. In our regime of ω, the thickness of the fluidized zone is increasing with increasing angular velocity [14, 15]. This means that for higher angular velocities the small particles need more time to segregate through the fluidized layer onto the solid block than for lower ω, therefore the final amount of segregation cannot be as good as for low values of ω. Even though the segregation speed is better for higher ω which is due to the greater throughput of material in the fluidized zone it will need more revolutions to achieve the saturated state than for lower angular velocities.

The effect of a larger fluidized zone on the final amount of segregation q_∞ and the initial segregation speed τ is demonstrated in the Figures 6a, 6b and 7 by adding some data points for $k_s = 50\,000$. The dotted line corresponds to the power law fits $\tau'(\omega) = 10.6\ \omega^{-0.6}$ and $n'_R = 1.69\ \omega^{0.4}$, respectively, which verifies that a larger fluidized layer corresponds to a faster

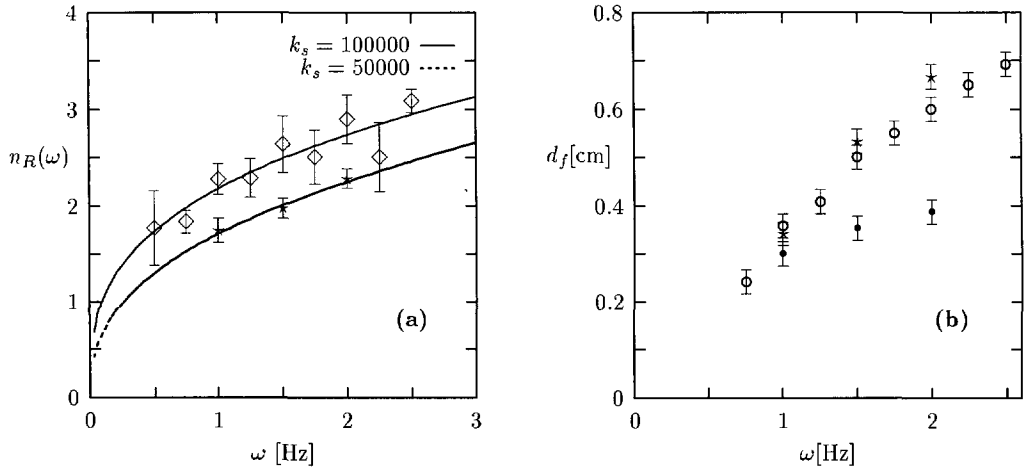

Fig. 7. — a) Number of characteristic revolutions n_R to achieve segregation and b) dependence of the thickness of the fuidized zone on k_s for the values $k_s = 50\,000(\star), 100\,000(\circ)$ and $150\,000(\bullet)$.

initial segregation speed (lower value of τ). But from Figure 6a, one also reads off that this means a lower value for the final amount of segregation. Thus decreasing the internal friction of the grains seems to have the same effect as increasing the rotation speed of the drum.

4. Conclusions

Radial segregation is well observed experimentally in rotating drums and we have studied its dynamics and its dependence on the external angular velocity of the drum and the thickness of the fluidized layer. We found that the quality of the segregation decreases with increasing angular velocity and the characteristic segregation time decreases. The latter seems to diverge in the limit $\omega \to 0$.

We speculate that in three spatial dimensions, radial segregation is more easily to achieve, since the empty spaces between the particles are connected by a network and small particles could traverse through it which will lead to a better segregation. Also in three dimensions small particles colliding with larger ones can be deflected parallel to the direction of the rotational axis and therefore the velocity in direction of the downwards flow is reduced. Hence the particles have more time to segregate until they hit the wall. These hypotheses could be tested by performing real three-dimensional numerical simulations and investigating the diffusion constants in different directions.

Acknowledgments

We would like to thank S. Grossmann for enlightening discussions and gratefully acknowledge financial support by the Deutsche Forschungsgemeinschaft and a generous grant of computer time by the HRZ Marburg.

References

[1] Jaeger Y, Nagel Y and Behringer R.P., *Phys. Today* **4** (1996) 32.
[2] Bridgewater J., *Powder Technol.* **15** (1976) 215.
[3] Cantelaube F. and Bideau D., *Europhys. Lett.* **30** (1995) 133.
[4] Clément E., Rajchenbach J. and Duran J., *Europhys. Lett.* **30** (1995) 7.
[5] Hill K.M. and Kakalios J., *Phys. Rev. E* **49** (1994) 3610; *Phys. Rev. E* **52** (1995) 4393.
[6] Cantelaube F., Ph.D. Thesis (Université de Rennes I, 1995).
[7] Ristow G.H., *Europhys. Lett.* **28** (1994) 97.
[8] Metcalfe Y, Shinbrot T., McCarthy J.J. and Ottino J.M., *Nature* **374** (1995) 39.
[9] Peratt B.A. and Yorke J.A., *Europhys. Lett.* **35** (1996) 31.
[10] Cundall Y and Strack O.D.L., *Géotechnique* **29** (1979) 47.
[11] Nakagawa M., private communications.
[12] Dury C.M. and Ristow G.H., Size Segregation in a Two Dimensional Rotating Drum, in "Friction, Arching, Contact Dynamics", D.E. Wolf and Grassberger, Eds. (World Scientific, Singapore in print).
[13] Baumann Y, Janosi I. and Wolf D., *Europhys. Lett.* **27** (1994) 203.
[14] Ristow G.H., *Europhys. Lett.* **34** (1996) 263.
[15] Nakagawa M., Altobelli S.A., Caprihan A., Fukushima E. and Jeong E.-K., *Experiments in Fluids* **16** (1993) 54.